Available online at www.sciencedirect.com
SCIENCE DIRECT®

Thin Solid Films 513 (2006) 264 – 268

thin solid films

www.elsevier.com/locate/tsf

Dielectric properties of nitric oxide-annealed gate oxides grown on nitrogen-implanted silicon substrates

Y.Y. Chen [a,b,*], C.H. Chien [c], J.C. Lou [c]

[a] Computer Science and Information Engineering, Yuanpei Institute of Science and Technology, Hsinchu, Taiwan, ROC
[b] Energy and Environment Research Laboratories, Industrial Technology Research Institute, Chutung, Hsinchu, Taiwan, ROC
[c] Institute of Electronics, National Chiao-Tung University, Hsinchu, Taiwan, ROC

Received 10 November 2004; received in revised form 1 August 2005; accepted 11 January 2006
Available online 28 February 2006

Abstract

The characteristics of nitric oxide (NO)-annealed nitrided gate oxides grown on nitrogen-implanted silicon substrates (NIS) were studied in this paper. It was found that nitrogen accumulation occurred near the interface after NO-annealing, while NIS-grown nitrided oxide produced a uniform nitrogen distribution in the dielectric bulk. Moreover, it was found that the dielectric reliability is strongly dependent on the dosages used for NIS preparation. NIS with dosages smaller than 10^{14} cm^{-2} was found not to suppress the oxidation rate and to degrade the dielectric reliability. On the other hand, the samples with a dosage of 10^{15} cm^{-2} not only exhibited a significantly reduced oxidation rate, making it suitable for growing oxides of multiple thicknesses in sub-3 nm technologies meeting the Systems on Chip requirement, but also improved the dielectric reliability. NO-annealed NIS-grown nitrided oxides depict superior dielectric reliability and this technique appears to be suitable to replace the traditional SiO_2 at 0.13 μm technology node and beyond.

Keywords: Nitric oxide (NO); Nitrogen-implanted silicon substrate (NIS); Nitrided oxide; Transmission electron microscopy; Secondary ion mass spectroscopy; Implantation; Gates oxides

1. Introduction

The continuous shrinkage of the dimensions of device features to below a quarter-micron requires highly reliable ultra-thin dielectric films of around 3 nm. In such a thin oxide regime, the breakdown and wearing out of dielectric films are key technological issues that must be addressed. As an alternative gate dielectric, nitrided oxides have drawn considerable attention due to their superior performance and reliability properties over conventional SiO_2 [1–8]. There are two different primary methods to incorporate nitrogen into gate dielectrics, (I) post-oxidation annealing, including ammonia (NH_3), nitrous oxide (N_2O) and NO-annealing, and (II) nitrogen ion implantation into the silicon substrate (NIS) prior to the growth of gate dielectrics. However, NH_3 annealing introduces an excessive amount of nitrogen into the gate oxide resulting in reduced carrier mobility along with an excessive amount of hydrogen, which degrades hot carrier immunity [1–3]. Another candidate for nitrogen incorporation, N_2O-annealing requires a much higher thermal budget in order to obtain sufficient nitrogen incorporation [4–6]. As a result, NO-annealing of the initial oxide is preferred in preparing nitrided oxide with sufficient thickness in a reasonable growth time, considering the self-limiting nature of the growth in an NO ambient [6–8].

On the other hand, many efforts, including oxygen, argon and nitrogen implantation are often used to grow multiple gate oxide thicknesses in one thermal cycle in order to meet the Systems on Chip (SoC) requirements [9–14]. Oxygen implantation prior to gate oxide growth can improve oxide quality and form multiple oxide thicknesses [9], but it seems unsuitable to the application of deep-submicron generation. Since oxygen implantation will enhance the oxidation rate, the final thickness cannot be scaled down. Reports on argon implantation [10] indicate that one of the concerns about the argon implantation technique is that the implantation damage caused by heavy mass

---

[*] Corresponding author. Computer Science and Information Engineering, Yuanpei Institute of Science and Technology, Hsinchu, Taiwan, ROC. Tel.: +886 3 5917995; fax: +886 3 5835338.
E-mail address: yungyu@itri.org.tw (Y.Y. Chen).

0040-6090/$ - see front matter © 2006 Elsevier B.V. All rights reserved.
doi:10.1016/j.tsf.2006.01.017

Table 1
EOT, TEM physical thickness and dielectric constant of NO-annealed NIS-grown nitrided oxides

NIS dosage (cm^{-2})	EOT (nm)	TEM (nm)	κ
w/o	2.49	2.6	4.0
10^{13}	2.57	2.7	4.1
10^{14}	2.52	2.7	4.1
10^{15}	1.97	2.3	4.6

argon ions may need a longer thermal cycle for annealing. In looking at the benefits and drawbacks of the available options, nitrogen implantation can be considered as a proper technology to meet the requirement of deep submicron devices [11–14]. Since nitrogen implantation can retard oxidation rate, it is more suitable to be implemented in SoC technology. Moreover, incorporated nitrogen can be used to suppress boron penetration [14–16], since it was observed not to be present in both the oxygen and argon implantation techniques. In this paper, the reliability characteristics of the NO-annealed NIS-grown nitrided oxides are studied. Although nitrided oxides degrade flat-band voltage shift and interface state density, the incorporation of nitrogen is demonstrated to effectively suppress trap generation and improve time-to-breakdown (t_{BD}).

2. Experimental details

Local oxidation of silicon (LOCOS) isolated metal-oxide-semiconductor (MOS) capacitors were fabricated on p-type (100) silicon wafers. After forming LOCOS isolation, nitrogen was implanted into the silicon substrates with 10 keV at the splitting dosages of 10^{13}, 10^{14} and 10^{15} cm^{-2}, which are defined as light, medium and heavy NIS dosages, respectively. In addition, some wafers without nitrogen implantation were used for comparison. Wafers were then cleaned and dipped in hydrofluoric (HF) acid before oxidation. The gate dielectrics were grown at 750 °C followed by NO-annealing at 850 °C for 1 h. Then 1500 Å polysilicon was deposited with in-situ doped phosphorus of 10^{20} cm^{-3}. Dopants were then activated at 950 °C for 30 s. After gate electrodes patterning and the etching of contact holes, aluminum metallization was done followed by sintering at 450 °C in N_2 ambient.

Square or circular capacitors of different areas, ranging from 2.5×10^{-5} to 1×10^{-2} cm^2, with LOCOS isolation were used to evaluate the integrity of the gate oxide. The physical gate oxide thickness was determined by high-resolution field emission transmission electron microscopy (HR-FETEM), JEOL-2010F. The equivalent oxide thickness (EOT) listed in Table 1 was extracted by fitting the measured high-frequency capacitance–voltage (*C–V*) data from HP4284 LCR meter under an accumulation condition with quantum mechanical correction [17,18]. The tunneling leakage current density–gate voltage (*J–V*) and the reliability characteristics of MOS capacitors were measured by Semiconductor Parameter Analyzer HP4145A. Nitrogen depth profiles and compositions were analyzed by CAMECA IMS-4f magnetic sector secondary ion mass spectroscopy (SIMS). The microroughness of the wafer surface and the interface between nitrided oxides/silicon were detected by tapping mode atomic force microscopy (AFM) D3100.

3. Results and discussion

Fig. 1(a) compares the *C–V* curves of the NO-annealed NIS-grown nitrided oxides. For light and medium NIS dosages, i.e., 10^{13} and 10^{14} cm^{-2}, no obvious difference in the *C–V* curves was observed. However, significant flat-band voltage (V_{FB}) shift and interface state density (D_{it}) increment were clearly evident for the nitrided oxide fabricated with heavy NIS dosages, i.e., 10^{15} cm^{-2}. Since nitrogen (N) is a donor-type impurity, the acceptor concentration in the substrate will be compensated by the implanted N atoms before oxidation, resulting in a smaller V_{FB} [11]. It is known that post-oxidation NO-annealing will introduce N into the gate oxides/substrate interface and, as a consequence, this will lead to the increased V_{FB} shift and D_{it} [19]. On the contrary, NIS before oxidation will reduce substrate doping and slightly recover the V_{FB} shift. The enhanced oxidation rates observed in the nitrided oxides with NIS dosages smaller than 10^{14} cm^{-2} are attributed to insufficient annealing because of the damage created by the ion bombardment, which in turn leads to smaller capacitances. With the heavy implant dosages of 10^{15} cm^{-2}, the growth rate was found to be reduced by nearly 15%, which seems substantially smaller than the numbers reported in Ref. [13], but this can probably be attributed to the lower oxidation temperature in our

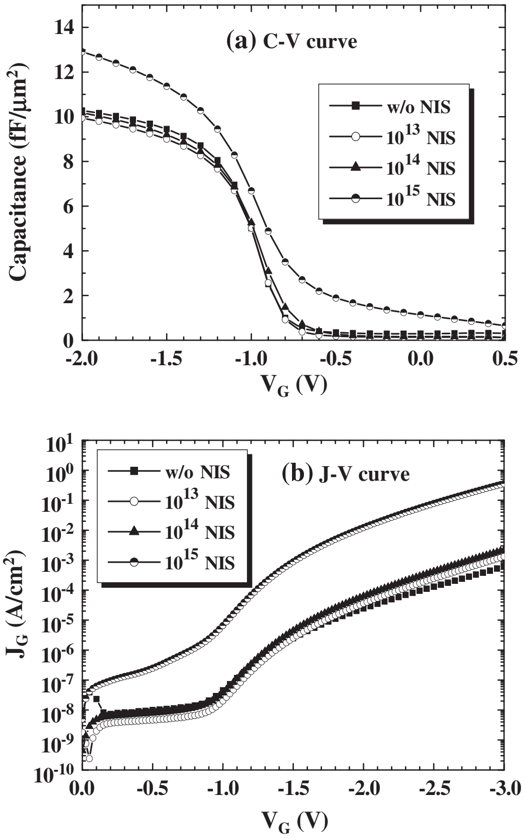

Fig. 1. (a) *C–V* curves and (b) *J–V* curves of NO-annealed NIS-grown nitrided oxides.

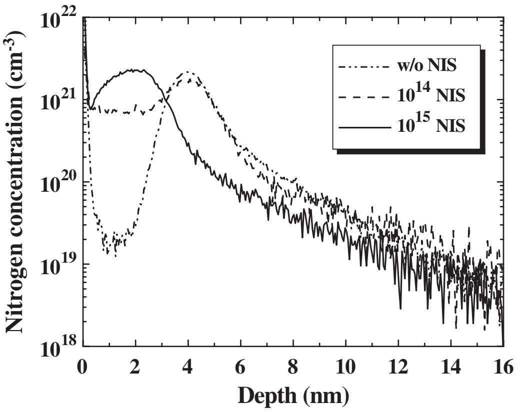

Fig. 2. SIMS nitrogen depth profiles of NO-annealed NIS-grown nitrided oxides.

study. Accompanying the increasing implantation dose, the dielectric constant (κ) was seen to increase from 4.0 of NO-annealed nitrided oxide to 4.6 of NO-annealed NIS-grown nitrided oxide and is summarized in Table 1. *J–V* curves for the NO-annealed NIS-grown nitrided oxides at negative gate bias are shown in Fig. 1(b). For the cases of 10^{13} and 10^{14} cm^{-2} dosages, the leakage current increases only slightly because of the residual implantation damages. Nevertheless, for the case of 10^{15} cm^{-2} dosages, the leakage current density increases more substantially because the oxidation rate is suppressed by the large amount of the nitrogen incorporation.

Fig. 2 indicates the nitrogen distribution profiles with and without NIS from SIMS analysis. Without NIS the dielectric bulk lacks nitrogen. After post-oxidation NO-annealing, more N will diffuse to interface and form $Si_3{\equiv}N$ bonds [20]. Moreover, the sample with 10^{15} cm^{-2} dosages not only exhibits higher peak concentration at the interface, but also has tighter N distribution than the samples with smaller NIS dosages. Fig. 3(a) compares the transient trapping behavior of NO-annealed NIS-grown nitrided oxides during constant current stress (CCS). It should be noted that all samples show apparent hole trapping characteristics. For dosages less than 10^{14} cm^{-2}, pre-oxidation nitrogen implantation will enhance the hole trapping. As the NIS dosages increase to 10^{15} cm^{-2}, the hole trapping becomes negligible. The trap generation rate as a function of injected charges is shown in Fig. 3(b). Eliminated trap generation rates are only visualized in samples with heavy N implantation, i.e., 10^{15} cm^{-2}. Fig. 4 presents the time-dependent dielectric breakdown (TDDB) Weibull distribution of NO-annealed NIS-grown nitrided oxides during constant voltage stress (CVS) at −4.3 V. Nitrided oxides with NIS dosages smaller than 10^{14} cm^{-2} reveal much poorer t_{BD} than the

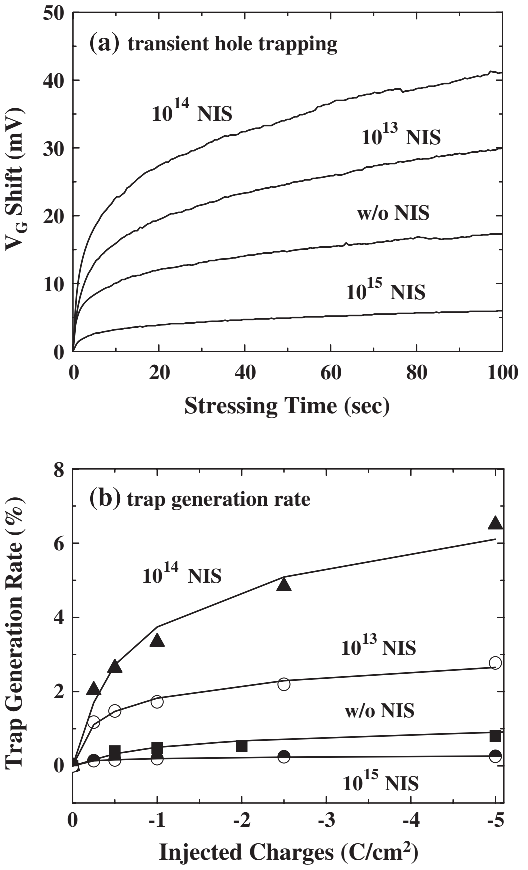

Fig. 3. (a) Transient hole trapping behaviors and (b) trap generation rates of NO-annealed NIS-grown nitrided oxides under −20 mA/cm^2 CCS.

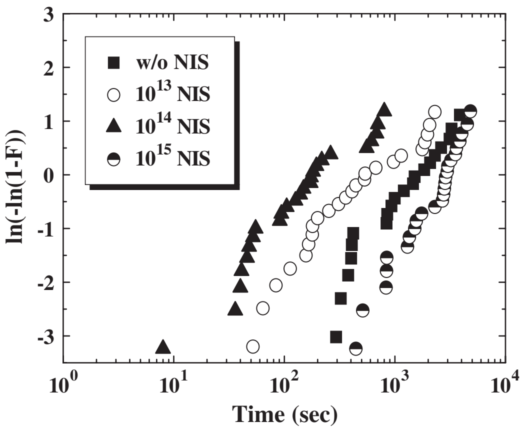

Fig. 4. t_{BD} Weibull distribution of NO-annealed NIS-grown nitrided oxides under −4.3 V CVS.

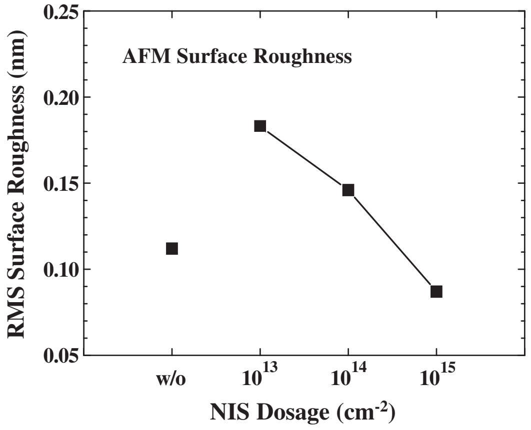

Fig. 5. Silicon surface roughness of NO-annealed NIS-grown nitrided oxides after the removal of the dielectrics.

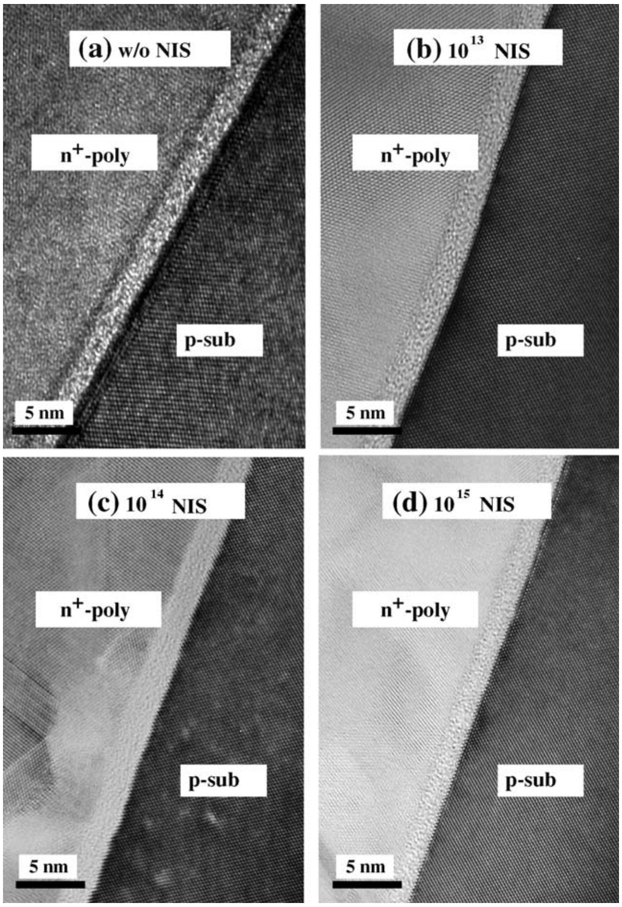

Fig. 6. HR-FETEM cross-sectional images of NO-annealed NIS-grown nitrided oxides.

samples without NIS, due to the larger hole-trapping generation rate. Consistent with the results as shown in Fig. 3, the sample with heavy NIS dosages is expected to exhibit the largest t_{BD}.

In this present study, NIS dosages less than 10^{14} cm^{-2} slightly increased the oxidation rate due to the insufficient post-oxidation annealing from damage caused by the ion bombardment, as shown in Fig. 1(a). The residual damage may increase the number of weak bonds during oxidation, and result in a worse stress-induced leakage current (SILC) immunity, enhanced trap generation rate and poor t_{BD}. Inferior surface roughness is also responsible for the degraded dielectric reliability, as seen in Fig. 5. On the other hand, the samples with 10^{15} cm^{-2} NIS dosages not only can be used to grow multiple oxide thickness, but they also produce a significant improvement in reliability. This trend is quite different from the results in the samples with lighter NIS dosages and can be due to several reasons. First, the surface is abounded with N atoms for heavy NIS implantation dosages, which may easily replace weak Si–O bonds, damaged by ion bombardment in the transition region, by strong $Si_3\equiv N$ bonds during oxidation. Second, implantation would change the interface morphology. From Fig. 5, it is evident that, despite NO-annealing being known for smooth surface morphology [19], roughness is increased when the NIS dosages increase from 0 to 10^{14} cm^{-2}, which may be due to the slightly faster oxidation rates from the damaged surface and less N area density. On the other hand, the surface becomes almost atomically flat when the NIS dosages are further increased to 10^{15} cm^{-2}. A smoother interface is helpful in reducing the localized field and hence results in stronger SILC immunity and larger t_{BD}. Cross-sectional TEM images are shown in Fig. 6. For heavy NIS dosages, the nitrided oxide/silicon interface is very smooth and there is a highly uniform transition region from the crystalline silicon to the amorphous nitrided oxide. This feature is beneficial to the electrical properties of the MOS device as described above. Third, it is known that SILC becomes negligible as the oxide thickness is scaled down to the direct-tunneling dominated regime. The heaviest NIS dosages can significantly retard the oxidation rate and grow the thinnest oxide, as shown in Fig. 1 (a). As a consequence, the nitrided oxides with NIS dosages of 10^{15} cm^{-2} cannot only grow multiple oxide thickness to meet SoC requirements, but also possess a stronger SILC immunity and better TDDB characteristics than others.

4. Conclusions

According to the International Technology Roadmap for Semiconductors, oxide thicknesses below 3 nm are necessary for the fabrication of deep sub-quarter micron devices. In the present study, an obvious oxidation rate retardation effect is observed only for the sample with heavy NIS dosages. The dielectric property is also strongly dependent upon the NIS dosages. NIS with dosages smaller than 10^{14} cm^{-2} is ineffective for oxidation rate suppression and degrades the dielectric reliability characteristic as well. On the other hand, the samples with 10^{15} cm^{-2} NIS dosages not only can be used to grow multiple oxide thickness to meet SoC requirements, but they also improve stress immunity. Nitrogen implantation also generates a uniformly distributed nitrogen profile in the dielectric bulk, which can be used as an effective diffusion barrier to resist against boron penetration. In conclusion, NO-annealed NIS-grown nitrided oxides can improve dielectric reliability, which are suitable for replacing traditional SiO_2 at 0.13 μm and beyond.

References

[1] Z.H. Liu, H.-J. Wann, P.K. Ko, C. Hu, Y.C. Cheng, IEEE Electron Device Lett. 13 (1992) 402.
[2] P. Pan, J. Appl. Phys. 61 (1987) 284.
[3] T. Hori, H. Iwasaki, K. Tsuji, IEEE Trans. Electron Devices 36 (1989) 340.
[4] G.W. Yoon, A.B. Joshi, J. Kim, D.L. Kwong, IEEE Electron Device Lett. 14 (1993) 179.
[5] T. Hori, Microelectron. Eng. 22 (1993) 245.
[6] E.P. Gusev, H.-C. Lu, E.L. Garfunkel, T. Gustafsson, M.L. Green, IBM J. Res. Develop. 43 (1999) 265.
[7] M. Fujiwara, M. Takayanagi, T. Shimizu, Y. Toyoshima, Tech. Dig., Int. Electron Devices Meet., San Francisco, U.S.A., Dec. 10–13, 2000, p. 227.
[8] T. Ohguro, Y. Okayama, K. Matsuzawa, K. Matsunaga, N. Aoki, K. Kojima, S. Momose, K. Ishimaru, Symp. VLSI Tech. Dig., Kyoto, Japan, June 10–12, 2003, p. 37.
[9] Y.-C. King, C. Kuo, T.-J. King, C. Hu, Tech. Dig., Int. Electron Devices Meet., San Francisco, U.S.A., Dec. 6–9, 1998, p. 585.

[10] M. Togo, K. Noda, T. Tanigawa, Tech. Dig., Int. Electron Devices Meet., San Francisco, U.S.A., Dec. 6–9, 1998, p. 347.

[11] A. Furukawa, Y. Abe, S. Shimizu, T. Kuroi, Y. Tokuda, M. Inuishi, Symp. VLSI Tech. Dig., Honolulu, U.S.A., June 11–13, 1996, p. 62.

[12] C.T. Liu, Y. Ma, M. Oh, P.W. Diodato, K.R. Stiles, J.R. McMacken, F. Li, C.P. Chang, K.P. Cheung, J.I. Colonel, W.Y.C. Lai, R. Liu, E.J. Lloyd, J.F. Miner, C.S. Pai, H. Vaidya, J. Frackoviak, A. Timko, F. Klemens, H. Maynard, J.T. Clemens, Tech. Dig., Int. Electron Devices Meet., San Francisco, U.S.A., Dec. 6–9, 1998, p. 589.

[13] L.K. Han, S. Crowder, M. Hargrove, E. Wu, S.H. Lo, F. Guarin, E. Crabbé, L. Su, Tech. Dig., Int. Electron Devices Meet., Washington, U.S.A., Dec. 7–10, 1997, p. 643.

[14] J.O. Bark, S.W. Kim, IEEE Electron Lett. 34 (1998) 1887.

[15] B. Yu, D.-H. Ju, W.-C. Lee, N. Kepler, T.-J. King, C. Hu, IEEE Trans. Electron Devices 45 (1998) 1253.

[16] Q. Xu, H. Qian, Z. Han, G. Lin, M. Liu, B. Chen, C. Zhu, D. Wu, IEEE Trans. Electron Devices 51 (2004) 113.

[17] K.J. Yang, C. Hu, IEEE Trans. Electron Devices 46 (1999) 1500.

[18] K. Yang, Y.-C. King, C. Hu, Symp. VLSI Tech. Dig., Kyoto, Japan, June 14–16, 1999, p. 77.

[19] B. Maiti, P.J. Tobin, V. Misra, R.I. Hegde, K.G. Reid, C. Gelatos, Tech. Dig., Int. Electron Devices Meet., Washington, U.S.A., Dec. 7–10, 1997, p. 651.

[20] T. Ogata, M. Inoue, T. Nakamura, N. Tsuji, K. Kobayashi, K. Kawase, H. Kurokawa, T. Kaneoka, Y. Ohno, H. Miyoshi, Tech. Dig., Int. Electron Devices Meet., San Francisco, U.S.A., Dec. 6–9, 1998, p. 597.